SSR Institute of International Journal of Life Sciences
ISSN (O): 2581-8740 | ISSN (P): 2581-8732
Bhattacherjee *et al*., 2026
doi: 10.21276/SSR-IIJLS.2026.12.2.20

Original Article

open access

Hepatoprotective Potential of Green-Synthesized CuO Nanoconjugate (*Raphanus sativus*) against Paracetamol-Induced Liver Toxicity in Mice

Satarupa Bhattacherjee[1], Indrajit Mandal[1], Manisha Kundu[1], Piyali Halder[1], Sukhen Das[1], Debasish Modak[2], Ruma Basu[3], Sandip Kumar Sinha[4], Birupaksha Biswas[5]*

[1]Dept of Physics, Jadavpur University, 188/Raja Subodh Chandra Mullick Road, Jadavpur, Kolkata, India
[2]Lakhotia Medical Centre, 268/2B, GT Road, Don Bosco, Howrah, India
[3]Dept of Physics, Jogomaya Devi College, 26 S.P. Mukherjee Road, Kolkata, India
[4]Dept of Human Physiology with Community Health, Vidyasagar University, Paschim Midnapore, India
[5]Dept of Pathology, Burdwan Medical College & Hospital, Purba Bardhaman, West Bengal, India

***Address for Correspondence:** Dr. Birupaksha Biswas, Consultant, Dept of Pathology, Burdwan Medical College & Hospital, Purba Bardhaman, West Bengal, India
E-mail: drbiswasmd@aol.com

Received: 15 Nov 2025/ Revised: 28 Dec 2025/ Accepted: 17 Feb 2026

ABSTRACT

Background: Paracetamol-induced hepatotoxicity is mediated by cytochrome P450–dependent formation of NAPQI, leading to glutathione depletion, oxidative stress, and hepatocellular injury. Green nanotechnology offers a sustainable approach to develop biocompatible therapeutics via plant-mediated nanoparticle synthesis. In this context, the present study focused on synthesizing CuO nanoconjugates using *Raphanus sativus* leaf extract and evaluating their hepatoprotective efficacy in a murine model.

Methods: CuO nanoparticles were synthesized using leaf extract via alkaline precipitation and characterized by XRD, FTIR, FESEM, EDX, HRTEM, and UV–Vis spectroscopy. Male Swiss albino mice (n=4/group) were allocated to six groups. Hepatotoxicity was induced with paracetamol (15 days), followed by treatment (15 days). Biochemical, hematological, oxidative stress (SOD, CAT, MDA), cytotoxicity (MTT), and histopathological analyses were performed (ANOVA, $p<0.05$).

Results: Monoclinic CuO (~27 nm) with phytochemical capping was confirmed. Nanoconjugates (30–40 nm) demonstrated superior hepatoprotection, normalizing bilirubin and transaminases (AST: 83.37→34.00 IU/L) comparable to silymarin. Antioxidant restoration (↑SOD, ↑CAT, ↓MDA), hematological recovery, high biocompatibility, and histological regeneration were observed.

Conclusion: *R. sativus*–derived CuO nanoconjugates exert potent antioxidant-mediated hepatoprotection, representing a promising, eco-friendly nanotherapeutic platform for liver disorders.

Key-words: Antioxidant activity, Biochemical biomarkers, CuO nanoconjugate, FTIR spectroscopy, Green synthesis, Histopathology, Hepatoprotection, Oxidative stress, Paracetamol toxicity, XRD analysis

INTRODUCTION

Nanomaterials possess unique physicochemical properties, including nanoscale size, high surface-to-volume ratio, and enhanced reactivity, enabling diverse applications in medicine, biotechnology, and environmental sciences [1,2].

How to cite this article
Bhattacherjee S, Mandal I, Kundu M, et al. Hepatoprotective Potential of Green-Synthesized CuO Nanoconjugate (*Raphanus sativus*) against Paracetamol-Induced Liver Toxicity in Mice. SSR Inst Int J Life Sci., 2026; 12(2): 9448-9458.

Access this article online
https://iijls.com/

Conventional synthesis methods often involve toxic reagents and high energy consumption, whereas green synthesis using biological sources offers a safe, eco-friendly, and cost-effective alternative [3,4].

Metal oxide nanoparticles such as ZnO, CeO_2, Fe_2O_3, and CuO have gained attention due to their broad physicochemical and biological properties [5,6]. Among them, CuO nanoparticles exhibit significant antimicrobial, catalytic, electrical, and optical characteristics, supporting applications in drug delivery, biosensing, and anticancer therapy [7,8]. Plant-mediated synthesis is particularly advantageous, as phytochemicals act as

doi: 10.21276/SSR-IIJLS.2026.12.2.20

reducing and stabilizing agents, improving nanoparticle stability and biocompatibility [4].

Drug-induced liver injury (DILI) remains a major clinical concern and a leading cause of acute liver failure [9]. Many drugs exhibit hepatotoxic potential, particularly at higher doses [10]. Paracetamol-induced hepatotoxicity occurs via CYP450-mediated formation of the toxic metabolite NAPQI, leading to glutathione depletion, oxidative stress, and hepatocellular damage [11].

Liver diseases represent a significant global burden, especially in developing countries such as India, where DILI is prevalent [12]. Jaundice is a common clinical manifestation associated with bilirubin accumulation. Silymarin is a well-established hepatoprotective agent with antioxidant and membrane-stabilizing properties [13]. However, plant-based alternatives such as *R. sativus* leaves, rich in flavonoids and phenolic compounds, also demonstrate hepatoprotective potential.

Therefore, the present study focuses on the green synthesis of CuO nanoparticles using *R. sativus* leaf extract and evaluates their hepatoprotective efficacy against paracetamol-induced liver injury, with emphasis on antioxidant and cytoprotective mechanisms.

MATERIALS AND METHODS

Fresh *R. sativus* leaves were authenticated (Department of Botany, Vidyasagar University). Paracetamol (Merck, India) was used for hepatotoxicity induction; silymarin (Zydus Cadila, India) served as the reference drug. Liver function assays were performed using Autospan (Merck India) diagnostic kits per manufacturer protocols.

Green Synthesis of Nano-conjugate

Preparation of aqueous plant extract- Fresh *R. sativus* leaves (200 g) were washed, air-dried, and cut into small pieces. The material was homogenized with 150 mL distilled water and heated for ~8 min. The mixture was filtered (Whatman No. 1) and the extract was stored at 4°C for further use [14].

Preparation of Green Synthesis of Copper oxide nanoparticle- CuO-NPs were synthesized using *R. sativus* leaf extract as a reducing and stabilizing agent. The extract was mixed with 0.1 M $CuSO_4$ and stirred for 15 min at room temperature. KOH was added dropwise to maintain pH 10–11, followed by overnight stirring for nanoparticle formation.

The precipitate was collected by centrifugation (10,000 rpm, 20 min), washed three times with distilled water, and dried at 80°C to obtain CuO nanoconjugate, which was used for further experimental evaluation [15].

Animal Preparation- Male Swiss albino mice (25–28 g) were procured from Saha Enterprise, Kolkata, and maintained as per CPCSEA guidelines (Reg. No. 50/CPCSEA/1999). Animals were divided into six groups (n=4) and housed in polypropylene cages under controlled conditions (20 ± 2°C, 45–60% humidity, 12 h light/dark cycle) with standard diet and water ad libitum. Animals were acclimatized for 7 days before the experiment. All procedures were approved by IAEC, Vidyasagar University (Approval No. VU/IAEC/CPCSEA/9/6/2022).

Characterization of Synthesized Nanoconjugate- The structural, morphological, and physicochemical properties of CuO-NPs were analyzed using XRD (Bruker D8, USA) for crystalline phase, crystallite size, and microstrain, and FTIR (PerkinElmer Spectrum 100, Germany) for functional groups. Surface morphology was examined by FESEM (Zeiss EVO-60), elemental composition by EDX, and detailed structure by HRTEM (JEOL JEM-2100, USA). Optical properties were studied using UV–Vis spectroscopy (PerkinElmer Lambda 365) [16,17].

Schematic representation of green synthesis of CuO nanoconjugate using *R. sativus* extract, including $CuSO_4$ reduction, KOH-mediated precipitation, purification, thermal stabilization, and characterization (XRD, FTIR, FESEM, EDX, HRTEM, UV–Vis), is shown in Fig. 1.

doi: 10.21276/SSR-IIJLS.2026.12.2.20

Fig. 1: Schematic representation of green synthesis and characterization of CuO nanoconjugate using *R. sativus* extract

Comparative treatments, including herbal extract, CuO nanoparticles, nanoconjugate, and silymarin enabling evaluation of relative hepatoprotective efficacy, with the nanoconjugate representing the integrated nano-bio therapeutic approach (Table 1).

Table 1: Table outlines the experimental design, where paracetamol induction (1–15 days) establishes hyperbilirubinemia, followed by targeted therapeutic interventions (16–30 days) across different treatment groups.

Group (n=4)	Induction Period (1-15 days)	Drug Administration (16-30 days)	Remarks
I	NA	NA	Control
II	Paracetamol (1 ml/kg BW)	NA	Hyperbilirubinemia
III	Paracetamol (1ml/kg BW)	*R. sativus* leaves extract (3 ml/ Kg BW)	Herb treated
IV	Paracetamol (1 ml/kg BW)	Cu-oxide nanoparticle (3 ml/ Kg BW)	Nanoparticle treated
V	Paracetamol (1 ml/kg BW)	Green Synthesized Nanoconjugate (copper oxide and *R. sativus*) (3 ml/ Kg BW)	Nanoconjugate treated
VI	Paracetamol (1 ml/kg BW)	Silymarin (3 ml/ Kg BW)	Clinical treated

Experimental animals were divided into six groups (n=4 per group) according to the treatment protocol described below.

Biochemical Estimation- Blood was collected from the retro-orbital plexus before sacrifice, allowed to clot for 45 min, and centrifuged at 6000 rpm for 15 min to obtain serum. Liver function was assessed by estimating ALT, AST, and other biochemical markers using standard kits [18].

Hematological Study- Blood was collected in heparinized tubes, and Hb, RBC, WBC, and platelet counts were determined using standard methods [19].

Biochemical Analysis- Liver tissues were homogenized in PBS (137 mM NaCl, 2.7 mM KCl, 10 mM Na_2HPO_4, 1.8 mM KH_2PO_4) and centrifuged at 8000 rpm for 10 min. The supernatant was used for SOD, MDA, and CAT estimation.

doi: 10.21276/SSR-IIJLS.2026.12.2.20

SOD Estimation- SOD activity was measured by the pyrogallol method using Tris buffer (50 mM, pH 8.2), 1 mM DTPA, 45 µL pyrogallol (10 mM), and 10 µL sample. OD was recorded at 420 nm and expressed as U/mg protein [20].

LPO (MDA) Estimation- 200 µL sample was mixed with 0.375% TBA and 15% TCA, heated at 95°C for 20 min, cooled, and extracted with 3 mL n-butanol. Absorbance was measured at 532 nm [21].

CAT Estimation- Catalase activity was measured using 0.1 mL homogenate, 1.9 mL buffer, and 1 mL H_2O_2. Decrease in absorbance was recorded at 240 nm and expressed as U/mg protein [22].

Cytotoxicity Study- Cell viability was assessed using the MTT assay [23].

Cell Morphology- Cells were isolated, centrifuged (10,000 rpm, 10 min), washed, treated with sucrose, recentrifuged (2000 rpm, 10 min), stained with EtBr/AO, incubated at 37°C for 20 min, and observed under fluorescence microscope [24].

Histopathological Study- Liver tissues were fixed in 10% formalin, dehydrated (50–100% ethanol), cleared in xylene, embedded in paraffin, stained with H&E, and examined microscopically [25].

Statistical Analysis- Data were expressed as Mean ± SEM and analyzed using one-way ANOVA ($p<0.05$).

RESULTS

The formation of CuO nanoparticles using *R. sativus* extract was confirmed by UV–Vis spectroscopy (200–800 nm), indicated by a greenish color change. A distinct absorption peak was observed at ~245 nm, corresponding to the surface plasmon resonance (SPR) of CuO nanoparticles (Fig. 2). The presence of a single peak suggests uniform and predominantly spherical nanoparticles, consistent with previous reports.

The XRD pattern of CuO nanoparticles showed peaks at 2θ values of 32.87°, 35.69°, 38.97°, 49.54°, 52.69°, 58.94°, and 61.46°, corresponding to monoclinic CuO (JCPDS No. 05-0661). The average crystallite size was calculated as ~27.33 nm using the Debye–Scherrer equation. The nanoconjugate exhibited broadened peaks indicating reduced crystallinity and the presence of an amorphous phase due to *R. sativus* extract (Fig. 3).

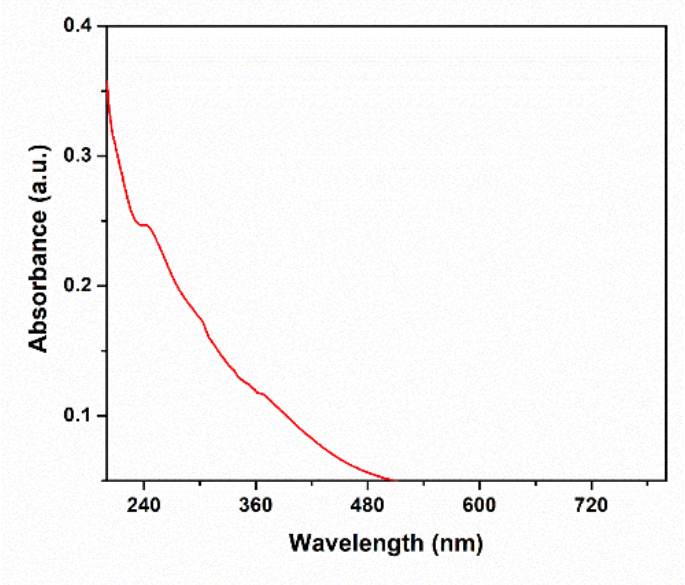

Fig. 2: UV–Vis spectrum of CuO nanoparticles showing absorption peak at ~245 nm

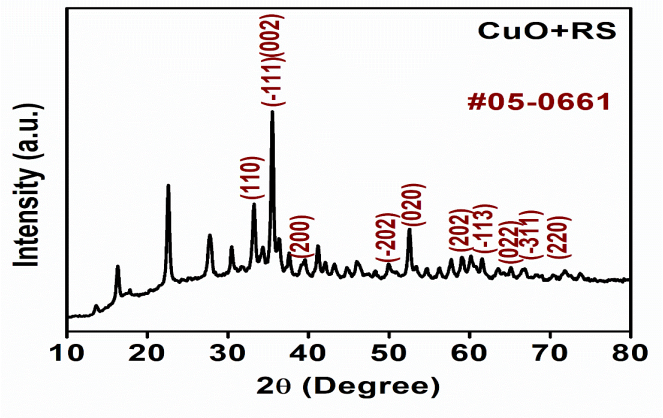

Fig. 3: XRD pattern showing coexistence of crystalline CuO nanoparticles and amorphous phase of *R. sativus* extract, with peak broadening indicating reduced crystallinity and nanoconjugate formation.

The FTIR spectrum of the synthesized sample shows distinct absorption bands within 500–700 cm^{-1}, indicating CuO nanostructures. Prominent peaks observed at 525, 584, and 672 cm^{-1} confirm the formation of CuO nanoparticles (Fig. 4). The peak at 525 cm^{-1} corresponds to Cu–O stretching (B_2u mode), which is consistent with XRD results, where the (202) plane represents Cu–O vibration.

doi: 10.21276/SSR-IIJLS.2026.12.2.20

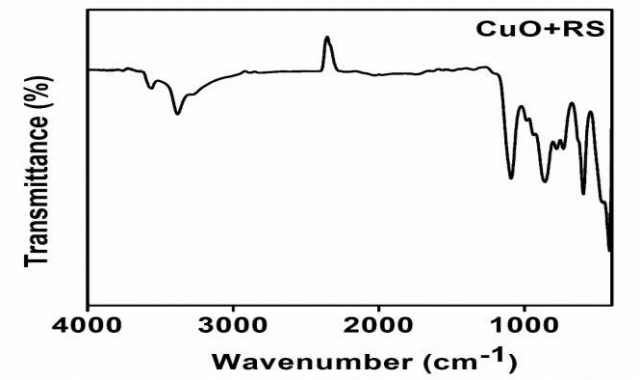

Fig. 4: FTIR spectrum showing characteristic Cu–O vibrational bands at 525, 584, and 672 cm^{-1} within 500–700 cm^{-1}, confirming the formation of CuO nanoparticles.

TEM analysis revealed slight agglomeration and predominantly spherical CuO nanoparticles with sizes ranging from 17–25 nm (Fig. 5a,b), consistent with XRD results. The nanoconjugate showed CuO nanoparticles enveloped by an amorphous organic matrix, with increased particle size of ~30–40 nm at different magnifications (Fig. 5), confirming successful conjugation and agreement with FESEM observations. The nanoscale size and spherical morphology may synergistically enhance biological activity, consistent with size- and shape-dependent nanotoxicological and antimicrobial effects.

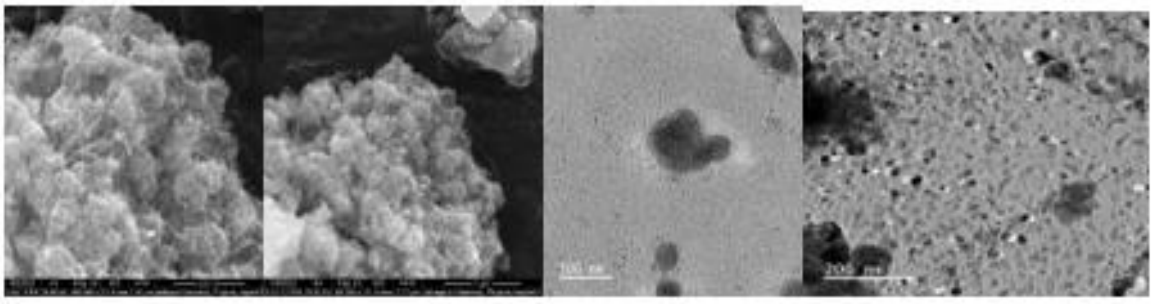

Fig. 5(From left to right): TEM/FESEM analyses reveal CuO nanoparticles encapsulated within an amorphous phytochemical matrix (~30–40 nm)

Body weight is a useful measure of health and can be used to assess the risk associated with paracetamol toxicity. A consistent loss in body weight is often the first indication of adverse effects. In the present study, male Swiss albino mice consumed a standard protein-rich diet during the acclimatization period, resulting in increased body weight and normal activity. However, after paracetamol administration, a reduction in body weight along with lethargic behavior was observed. Gradual recovery in body weight and activity was noted upon treatment with the green-synthesized nanoconjugate. The trend of body weight changes is presented in Table 2.

Table 2: Effects of Nanoconjugate on weight changes of paracetamol intoxicated mice in three conditions

Group (n=4)	Normal Condition	After Induction	After Treatment
Control	26.53±0.38	27.83±0.02	28.76±0.19
Autorecovary	25.43±0.09	25.58±0.20	25.83±0.03
HerbTreated	23.42±0.09	23.80±0.07	25.70±0.34
Nanoparticle Treated	25.87±0.60	25.14±0.03	26.79±0.56
Nanoconjugate	26.55±0.28	26.75±0.12	28.57±0.06
Silymarin Treated	26.57±0.23	26.30±0.42	27.73±0.26

All data is represented as Mean ±SEM, P values Calculated by ANOVA test, Test of Significance p<0.05 implies.

doi: 10.21276/SSR-IIJLS.2026.12.2.20

Serum biochemical parameters (bilirubin, AST, ALT, ALP, albumin, globulin, and total protein) were significantly altered in the autorecovery group compared to control. Treatment with herb, nanoparticles, and silymarin improved these parameters, while the nanoconjugate-treated group showed maximum restoration towards normal levels (Table 3).

Table 3: Effects of nanoconjugate on Liver enzyme of paracetamol intoxicated mice

Name of the Parameter(n=4)	Control	Auto recovery	Herb Treated	Nanoparticle Treated	Nanoconjugate Treated	Silymarin Treated
Bilirubin (mg/dl)	0.33±0.17	01.72±0.02	0.62±0.03	0.89±0.04	0.41±0.14	0.44±0.27
AST(IU/L)	25.50±1.2	83.37±1.17	45.11±3.77	40.50±1.29	34.00±1.91	41.5±4.65
ALT(IU/L)	26.50±0.816	84.57±5.34	46.50±1.707	57.50±0.72	54.50±1.852	61.5±0.957
ALP(IU/L)	91.50±1.29	115.67±1.1	94.25±3.77	97.00±1.82	90.75±0.95	96.75±2.9
GGT(IU/L)	2.620±0.11	7.77±0.16	4.67±0.13	5.41±0.72	3.65±0.12	3.17±0.33
Albumin (g/dl)	4.20±0.01	2.21±0.08	3.22±0.09	4.69±0.14	5.24±0.46	5.76±0.20
Globulin (g/dl)	2.80±0.56	1.49±0.58	5.50±0.18	3.57±0.23	3.31±0.19	5.68±0.17
Total Protein (g/dl)	7.5±0.78	3.5±0.862	4.5±0.42	4.3±0.24	6.8±0.21	6.6±0.20

All data is represented as Mean ±SEM, P values Calculated by ANOVA test, Test of Significance p<0.05 implies

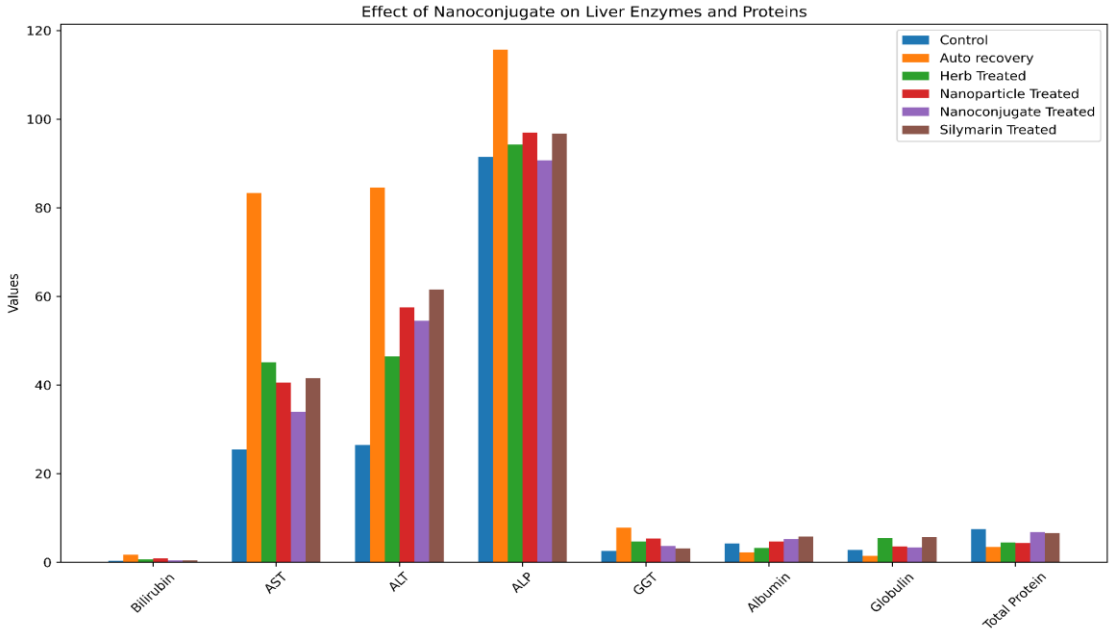

Fig. 6: The bar diagram illustrates the comparative effects of different treatment groups on key hepatic biochemical parameters in paracetamol-induced toxicity

Hematological parameters showed that Hb%, RBC, and platelet counts were decreased in the autorecovery group, while WBC levels were increased compared to control. Treatment with nanoconjugate significantly ($p<0.05$) improved Hb%, RBC, and platelet counts and reduced WBC levels towards normal (Table 4).

doi: 10.21276/SSR-IIJLS.2026.12.2.20

Table 4: Effect of nanoconjugate on hematological parameters of paracetamol intoxicated mice

Hematological parameters (n=4)	Control	Autorecovary	Herb Treated	Nanoparticle Treated	Nanoconjugate Treated	Silymarin Treated
Hb% (g/dl)	14.22±0.28	8.52±0.26	10.39±0.34	12.79±0.52	13.13±0.69	11.79±0.41
RBC (million/mm^3)	7.43±0.41	4.55±0.66	4.74±0.19	6.4±0.33	6.25±0.21	5.47±0.35
Platelet(lakhs/cumm)	352.25±1.7	264.25±2.0	274.25±2.0	283.75±1.98	324.25±1.5	275.75±2.0
WBC (mm^3)	3±0.3	6.5±0.75	5.7±0.58	5.8±0.58	4.1±0.75	4.6±0.59

All data is represented as Mean ±SEM, p-values calculated by ANOVA test, Test of Significance p<0.05 implies

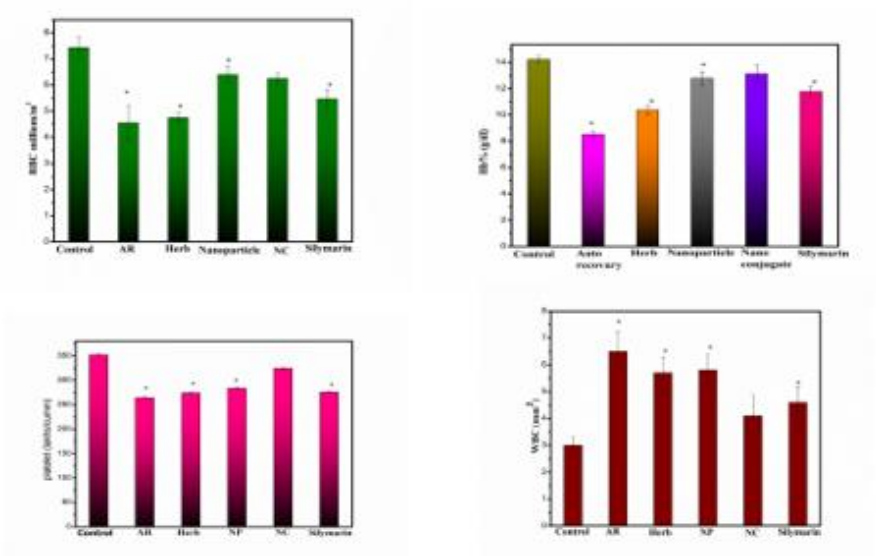

Fig. 7: Effect of nanoconjugate on haematological parameters of paracetamol intoxicated mice.

Oxidative stress markers showed that SOD and CAT levels were decreased, while MDA levels were increased in the paracetamol-treated (autorecovery) group compared to control. Treatment with nanoconjugate significantly improved SOD and CAT levels and reduced MDA levels ($p<0.05$), restoring them towards normal (Table 5).

Table 5: Effect of nanoconjugate on ROS parameters of Paracetamol intoxicated mice

Group n=4	Design of the treatment	SOD (µ/gm wt tissue)	MDA (µ/gm wt tissue)	CAT (µ/gm wt tissue)
Group-I	Control	3.68±0.22	17.53±1.63	6.61±0.05
Group -II	Auto recovery	2.67±0.33	48.33±1.02	2.59±0.36
Group-III	Herb Treated	3.74±0.24	30.39±0.97	4.69±0.33
Group-IV	Nanoparticle Treated	2.88±0.10	34.31±0.72	3.69±0.14
Group-V	Nanoconjugate Treated	3.71±0.29	27.02±0.90	6.80±0.20
Group-VI	Silymarin Treated	3.56±0.27	26.87±0.13	5.75±0.29

All data is represented as Mean ±SEM, P values calculated by ANOVA test, Test of Significance p<0.05 implies

doi: 10.21276/SSR-IIJLS.2026.12.2.20

CuO nanoconjugate treatment markedly reduced oxidative stress in paracetamol-induced mice by lowering lipid peroxidation levels. It also restored antioxidant enzyme activities (SOD and CAT), indicating improved hepatic defense against ROS (Fig. 8).

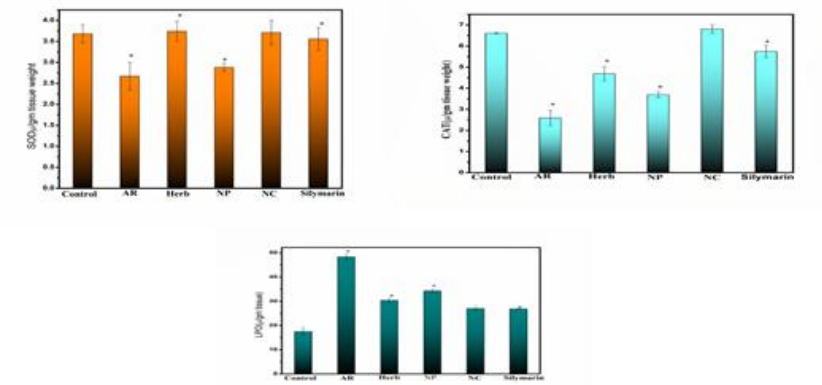

Fig. 8: Effect of nanoconjugate on ROS parameters of paracetamol-intoxicated mice.

Paracetamol-treated liver cells showed significant damage, indicated by red fluorescence, whereas treatment with green synthesized CuO nanoconjugate resulted in improved cell viability with increased green fluorescence (Fig. 9). This indicates the protective and regenerative effect of the nanoconjugate on damaged liver cells.

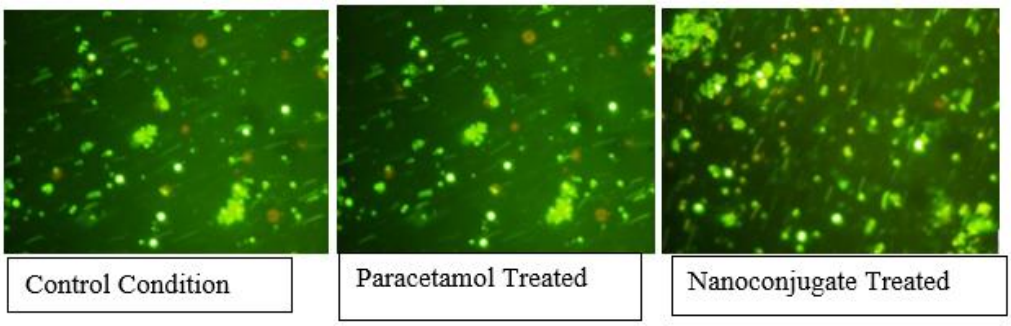

Fig. 9: Paracetamol-induced hepatocellular damage (red fluorescence) is markedly reduced upon treatment with green-synthesized CuO nanoconjugate, as indicated by increased viable cells (green fluorescence), demonstrating effective cytoprotection and cellular recovery.

The control group showed normal hepatic architecture with intact hepatocytes and no pathological changes. The paracetamol-treated group exhibited severe liver damage, including central vein congestion and neutrophilic infiltration. Treatment with nanoconjugate reduced hepatic injury, as indicated by decreased inflammation and vascular congestion in a dose-dependent manner, suggesting hepatocellular protection and recovery (Fig. 10).

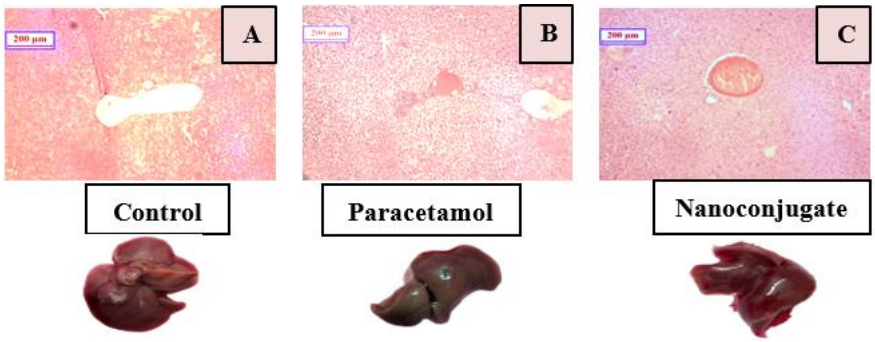

Fig. 10: Histopathological analysis further substantiated the biochemical findings.

doi: 10.21276/SSR-IIJLS.2026.12.2.20

DISCUSSION

The present investigation demonstrates that green-synthesized CuO nanoconjugates derived from *R. sativus* leaf extract exert significant hepatoprotective activity against paracetamol-induced liver injury, supported by structural characterization, biochemical biomarkers, oxidative stress indices, and histopathological observations. The integration of phytochemical constituents with metal oxide nanostructures provides a biologically compatible nanoplatform capable of modulating oxidative stress–mediated hepatocellular damage.

XRD analysis confirmed the formation of crystalline monoclinic CuO nanoparticles, consistent with the standard diffraction profile of CuO materials. The calculated crystallite size (~27 nm) lies within the nanoscale range reported to exhibit enhanced biological reactivity due to increased surface area and catalytic activity. Comparable crystallographic characteristics have been documented in plant-mediated CuO nanoparticle synthesis studies, where phytochemicals act as reducing and stabilizing agents during nanoparticle formation [26,27]. The broadened peaks observed in the nanoconjugate further suggest a partial amorphous coating derived from *R. sativus* phytochemicals, which may enhance nanoparticle dispersion and biological interaction.

FTIR analysis verified the characteristic Cu–O stretching vibrations in the 500–700 cm^{-1} region, confirming the formation of CuO nanostructures. Additionally, the presence of functional groups associated with plant metabolites indicates surface functionalization of nanoparticles by phytochemical components. Such plant-derived capping agents have been shown to improve nanoparticle stability, reduce aggregation, and enhance biological compatibility while imparting intrinsic antioxidant properties [28].

Morphological analysis using TEM and FESEM demonstrated predominantly spherical nanoparticles ranging from 17–25 nm, which increased to approximately 30–40 nm following nanoconjugate formation due to phytochemical encapsulation. Particle size and morphology play critical roles in determining nanoparticle biological performance, influencing cellular uptake, catalytic activity, and interaction with biomolecules [29]. Nanoparticles within the 20–40 nm range have been reported to exhibit optimal cellular interaction and improved therapeutic performance compared with larger particles [30].

The in vivo findings further revealed that paracetamol intoxication produced significant hepatic dysfunction characterized by elevated serum transaminases, bilirubin, and ALP levels, reflecting hepatocellular injury and metabolic disruption. Treatment with the green-synthesized nanoconjugate markedly restored these biochemical parameters toward physiological levels, demonstrating hepatoprotective efficacy comparable to the reference hepatoprotective compound silymarin. Paracetamol-induced hepatotoxicity is primarily mediated by the formation of the toxic metabolite N-acetyl-p-benzoquinone imine (NAPQI), which depletes intracellular glutathione and induces oxidative stress–mediated cellular injury [31].

Consistent with this mechanism, oxidative stress analysis revealed significant restoration of antioxidant enzymes (SOD and CAT) and reduction of lipid peroxidation marker MDA in nanoconjugate-treated animals. These findings suggest that the hepatoprotective effect of the nanoconjugate is largely mediated through reactive oxygen species (ROS) scavenging and enhancement of endogenous antioxidant defense systems. Previous investigations have reported that biofunctionalized metal oxide nanoparticles possess strong redox-regulatory capabilities and can effectively mitigate oxidative cellular damage [32].

Hematological parameters also showed notable improvement following nanoconjugate administration, including restoration of hemoglobin levels, RBC counts, platelet counts, and normalization of elevated WBC levels induced by paracetamol toxicity. These results indicate that the nanoconjugate may exert systemic protective effects by attenuating inflammatory responses and restoring physiological homeostasis [33].

Histopathological examination strongly supported these biochemical findings. Severe hepatic damage observed in paracetamol-treated mice, which do include inflammatory infiltration, sinusoidal congestion, and hepatocyte degeneration, was substantially ameliorated following nanoconjugate treatment. Restoration of hepatic architecture and reduced inflammatory infiltration indicate effective hepatocellular protection and tissue regeneration, consistent with previous reports highlighting the therapeutic potential of phytochemical-

doi: 10.21276/SSR-IIJLS.2026.12.2.20

mediated nanomaterials in oxidative liver injury models [34].

Collectively, the findings demonstrate that green-synthesized CuO nanoconjugates integrate the physicochemical advantages of nanomaterials with the biological activity of plant-derived antioxidants, resulting in enhanced hepatoprotective and antioxidative effects. This eco-friendly nanobiotechnological strategy may therefore represent a promising platform for the development of biocompatible, cost-effective nanomedicine approaches for the management of oxidative stress–related liver disorders.

CONCLUSIONS

The present study successfully demonstrated the green synthesis of CuO nanoconjugates using Raphanus sativus leaf extract, where phytochemicals acted as reducing and stabilizing agents. The synthesized nanoparticles exhibited controlled size, spherical morphology, and desirable physicochemical properties, as confirmed by multiple characterization techniques. Biological evaluation revealed that the nanoconjugate significantly attenuated paracetamol-induced hepatotoxicity by restoring biochemical, hematological, and oxidative stress parameters toward normal levels. Furthermore, histopathological and cellular studies confirmed its protective and regenerative effects on liver tissue. Overall, the findings suggest that the green-synthesized CuO nanoconjugate possesses promising hepatoprotective and antioxidant potential, making it a viable candidate for future therapeutic applications.

CONTRIBUTION OF AUTHORS

Research concept- Satarupa Bhattacherjee, Indrajit Mandal

Research design-Indrajit Mandal, Manisha Kundu

Supervision- Sandip Kumar Sinha, Birupaksha Biswas

Materials- Piyali Halder, Sukhen Das, Debasish Modak

Data collection- Piyali Halder, Sukhen Das, Debasish Modak, Ruma Basu

Data analysis and interpretation- Sandip Kumar Sinha, Birupaksha Biswas

Literature search- Satarupa Bhattacherjee, Indrajit Mandal

Writing article- Indrajit Mandal, Manisha Kundu, Piyali Halder

Critical review- Sandip Kumar Sinha, Birupaksha Biswas

Article editing- Satarupa Bhattacherjee, Indrajit Mandal, Manisha Kundu

Final approval- Sandip Kumar Sinha, Birupaksha Biswas

REFERENCES

[1] Khan I, Saeed K, Khan I. Nanoparticles: properties, applications and toxicities. Arab J Chem., 2019; 12(7): 908-31.

[2] Jeevanandam J, Barhoum A, Chan YS, Dufresne A, et al. Review on nanoparticles and nanostructured materials: history, sources, toxicity and regulations. Beilstein J Nanotechnol., 2018; 9: 1050-74.

[3] Shah M, Fawcett D, Sharma S, Tripathy SK, Poinern GEJ. Green synthesis of metallic nanoparticles via biological entities. Materials (Basel)., 2015; 8(11): 7278-08.

[4] Vanlalveni C, Lallianrawna S, Biswas A, Selvaraj M, Changmai B, et al. Green synthesis of silver nanoparticles using plant extracts and their antimicrobial activities: a review of recent literature. RSC Adv., 2021; 11(5): 2804-37.

[5] Sánchez-López E, Gomes D, Esteruelas G, et al. Metal-based nanoparticles as antimicrobial agents: an overview. Nanomaterials (Basel)., 2020; 10(2): 292.

[6] Vijayaram S, Razafindralambo H, Sun YZ, et al. Applications of green synthesized metal nanoparticles - a review. Biol Trace Elem Res., 2024; 202(1): 360-86.

[7] Naz S, Gul A, Zia M, Javed R. Synthesis, biomedical applications, and toxicity of CuO nanoparticles. Appl Microbiol Biotechnol., 2023; 107(4): 1039-61.

[8] Woźniak-Budych MJ, Staszak K, Staszak M. Copper and copper-based nanoparticles in medicine-perspectives and challenges. Molecules., 2023; 28(18): 6687.

[9] Molahalli V, Sharma A, Bijapur K, Soman G, Shetty A, et al, Chattham N, Hegde G, et al. Copper-based nanomaterials in organic transformations. ACS Symp Ser., 2024; 1-33.

[10] Makarov VV, Love AJ, Sinitsyna OV, et al. "Green" nanotechnologies: synthesis of metal nanoparticles using plants. Acta Nature, 2014; 6(1): 35-44.

[11] Andrade RJ, Chalasani N, Björnsson ES, et al. Drug-induced liver injury. Nat Rev Dis Primers, 2019; 5(1): 58.

doi: 10.21276/SSR-IIJLS.2026.12.2.20

[12]Hinson JA, Roberts DW, James LP. Mechanisms of acetaminophen-induced liver necrosis. Handb Exp Pharmacol., 2010; 196: 369-05.

[13]Du K, Ramachandran A, Jaeschke H. Oxidative stress during acetaminophen hepatotoxicity: sources, pathophysiological role and therapeutic potential. Redox Biol., 2016; 10: 148-56.

[14]Nortjie E, Basitere M, Moyo D, Nyamukamba P. Extraction methods, quantitative and qualitative phytochemical screening of medicinal plants for antimicrobial textiles: a review. Plants (Basel)., 2022; 11(15): 2011.

[15]Shang J, Zhou Q, Wang K, Wei Y. Engineering of green carbon dots for biomedical and biotechnological applications. Molecules., 2024; 29(18): 4508.

[16]National Research Council. Guide for the care and use of laboratory animals. Washington DC: National Academies Press, 2011.

[17]Mokari A, Guo S, Bocklitz T. Exploring the steps of infrared spectral analysis: pre-processing, data modelling and deep learning. Molecules., 2023; 28(19): 6886.

[18]Khan MSI, Oh SW, Kim YJ. Power of scanning electron microscopy and energy dispersive X-ray analysis in rapid microbial detection and identification at the single cell level. Sci Rep., 2020; 10(1): 2368.

[19]Giannini EG, Testa R, Savarino V. Liver enzyme alteration: a guide for clinicians. CMAJ., 2005; 172(3): 367-79.

[20]Yu D, Yam VW. Controlled synthesis of monodisperse silver nanocubes in water. J Am Chem Soc., 2004; 126(41): 13200-01.

[21]Kaplowitz N. Drug-induced liver injury. Clin Infect Dis., 2004; 38 Suppl 2: S44-S48.

[22]Regev A. Drug-induced liver injury and drug development: industry perspective. Semin Liver Dis., 2014; 34(2): 227-39.

[23]Mosmann T. Rapid colorimetric assay for cellular growth and survival. J Immunol Methods, 1993; 65(1-2): 55-63.

[24]Ribble D, Goldstein NB, Norris DA, Shellman YG. A simple technique for quantifying apoptosis in 96-well plates. BMC Biotechnol., 2005; 5: 12.

[25]Bancroft JD, Gamble M. Theory and practice of histological techniques. 6th ed. Churchill Livingstone; 2008.

[26]Hughes KJ, Ganesan M, Tenchov R, et al. Nanoscience in action: emerging trends in materials and applications. ACS Omega., 2025; 10(8): 7530-48.

[27]Usman O, Baig MM, Ikram M, et al. Green synthesis of metal nanoparticles and their anti-pathogenic properties. Sci Rep., 2024; 14(1): 11354.

[28]Rahuman HBH, Dhandapani R, Narayanan S, et al. Medicinal plants mediated green synthesis of silver nanoparticles and biomedical applications. IET Nanobiotechnol., 2022; 16(4): 115-44.

[29]Nel A, Xia T, Mädler L, Li N. Toxic potential of materials at nanolevel. Sci., 2006; 311(5761): 622-27.

[30]Albanese A, Tang PS, Chan WC. Effect of nanoparticle size, shape and surface chemistry on biological systems. Annu Rev Biomed Eng., 2012; 14: 1-16.

[31]Jaeschke H, Ramachandran A. Oxidant stress and lipid peroxidation in acetaminophen hepatotoxicity. React Oxyg Species., 2018; 5(15): 145-58.

[32]Lewin M, Carlesso N, Tung CH, et al. Tat peptide-derivatized magnetic nanoparticles for *in vivo* tracking. Nat Biotechnol., 2000; 18(4): 410-14.

[33]Kermanizadeh A, Gaiser BK, Hutchison GR, Stone V. In vitro liver model for oxidative stress and genotoxicity of nanomaterials. Part Fibre Toxicol., 2012; 9: 28.

[34]Sahu R, Goswami S, Narahari Sastry G, Rawal RK. Preventive and therapeutic potential of flavonoids in liver cirrhosis. Chem Biodivers., 2023; 20(2): e202201029.